Journal of Applied Pharmaceutical Research
Volume 14 Issue 1, Year of Publication 2026, Page 85 – 97
DOI: https://doi.org/10.69857/joapr.v14i1.1593

Check for updates

Research Article

JOURNAL OF APPLIED PHARMACEUTICAL RESEARCH | JOAPR
www.japtronline.com ***ISSN: 2348 – 0335***

FORMULATION, PHYSICOCHEMICAL CHARACTERIZATIONS, AND STABILITY PROFILING OF PALBOCICLIB-LOADED POLYMERIC NANOPARTICLE WITH ANTIOXIDANT AND ANTI-INFLAMMATORY INVESTIGATION FOR BREAST CANCER TREATMENT

Nurjamal Hoque, Ananta Choudhury*

Article Information
Received: 25th August 2025
Revised: 2nd November 2025
Accepted: 6th December 2025
Published: 4th January 2026

Keywords
Chitosan nanoparticle, Folic acid targeting, Palbociclib Nanoparticle, Stability of Palbociclib Nanoparticle, Anti-oxidant, Anti-inflammatory, Cytotoxicity

ABSTRACT
Background: Breast cancer is a highly prevalent malignancy worldwide with significant mortality, and conventional chemotherapy is often constrained by poor solubility, non-targeted distribution, and systemic toxicity, necessitating improved therapeutic approaches. **Methodology:** Palbociclib-loaded nanoparticles were formulated using chitosan, PVA, and sodium tripolyphosphate, characterized physicochemically, and evaluated for compatibility, bioactivity, stability, and MCF-7 cytotoxicity via MTT assay. **Results and Discussion:** PNs loaded with Palbociclib showed λmax at 342 nm, which was significantly linear between the range of 5−40 µg/ml (R^2 = 0.997). The particle size was 237.8 ± 1.76 nm, the PDI was 0.221, and the zeta potential was +34.09 ± 3.38 mV. The encapsulation efficiency and drug loading were 81.21 ± 1.80% and 43.0 ± 1.64%, respectively. The release was more sustained at pH 5.4 (93.25 ± 0.95%) than at pH 7.4 (80.78 ± 1.51%) after 24 h ($p < 0.0001$). The antioxidant activity (DPPH IC_{50} = 0.52 µg/ml) and anti-inflammatory activity (IC_{50} = 38.9 µg/ml) were better than free palbociclib (2.041 and 137.87 µg/ml). There was no significant change in the size (240.14 ± 1.91 nm), the PDI 0.283, the zeta potential +30.01 ± 2.68 mV, the loading of the drug (40.1 ± 1.58%), and the entrapment efficiency (79.02 ± 2.69%) after three months. PB-PNs resulted in a more pronounced proliferation inhibition effect in MCF-7 cells (IC_{50} = 5.85 µg/ml) as compared to the free palbociclib (18.15 µg/ml).**Conclusion:** The developed PB-PNs constitute a stable, pH-responsive, and enhanced anticancer therapy, meriting further *in vivo* investigation.

INTRODUCTION

The second-leading cause of death from cancer in women is breast cancer [1]. There is a desperate call for new approaches to screen for primary and metastasized breast cancer, which would help in increasing the patients' survival rates [2]. Investigations have shown that combining biocompatible and functionalized nanoparticles may be beneficial for combating cancerous growths [3], [4]. Polymer-based nanoparticles have

*Faculty of Pharmaceutical Science, Assam down town University, Sankar Madhab Path, Gandinagar, Panikhaiti, Guwahati, Assam 781026, India

For Correspondence: **anantachoudhury@gmail.com**

been investigated as an alternative to conventional chemotherapy, offering reduced side effects and improved therapeutic efficacy when loaded with anticancer agents [5], [6].

Polymeric nanoparticles can be made out of a variety of natural or synthetic polymers: alginate, gelatin, chitosan, poly(lactic acid-co-glycolic acid) (PLGA), poly(L-lactide) (PLA), and polycaprolactone (PCL) are only a few examples[7]. With the use of several synthetic chemotherapeutic drugs recently in the treatment of cancer, most of them present significant disadvantages, namely high toxicity, strong side effects, and a lack of sufficient qualities for the selective distribution of the drug [8]. Pfizer exploited the shortcomings in breast cancer therapy for the development of the targeted chemotherapeutic agent, palbociclib. Palbociclib is a selective inhibitor of cyclin-dependent kinase 4/6, used for the treatment of advanced breast cancer[9],[10].

Adverse reactions also include neutropenia, leukopenia, anaemia, and fatigue. Despite the toxicities observed in the lungs, liver, reproductive organs, and fetus, PLBs' primary associations are with off-target delivery. Resistance to administered chemotherapeutic drugs is increasingly common because the P-gp efflux pump expels anticancer drugs from cancer cells [11].

Polymeric Nanoparticles constitute a pioneering class of nanovehicles that can serve as innovative drug carriers and, simultaneously, versatile molecular tracking reporters to assist in delivering drugs to specific tissues [12]. The International Council for Harmonisation of Technical Requirements for Pharmaceuticals for Human Use (ICH) has outlined general guidelines for the preclinical stage of human new drug development and a comprehensive procedure for the stability study of the drug under investigation [13]. Thermal stability is typically assessed between 4 and 37 °C, and long-term storage stability should be evaluated for at least 1 year. Finding out which environmental elements - such as temperature [14], humidity [15], reactive oxygen species [15], and light [13]- contribute to the degradation of medicinal products is the aim. This aids in determining storage conditions that minimize degradation and preserve medication quality over time, in contrast to other types of pharmaceuticals [13]. Nanoformulations are evaluated for physical or colloidal stability. Both pharmaceutical stability over extended periods and chemical stability have been investigated [16].

MATERIALS AND METHODS

Materials

Palbociclib was generously provided by Natco Pharma in Hyderabad. Chitosan, acetone, ethanol, and polyvinyl alcohol were purchased from Loba Chemie Pvt. Ltd., Mumbai, Maharashtra, India. All chemicals and the active pharmaceutical ingredient (API) used in the present study were of analytical grade.

Method

Drug-Excipients Interactions by Fourier Transform Infra-Red (FTIR) spectroscopy

Drug analysis was performed using a Bruker Alpha II FTIR spectrometer. The samples with 1:1 ratios included lyophilised forms of palbociclib and chitosan, together with polyvinyl alcohol, as well as physical mixtures of the three components, made with or without drug incorporation [17][18].

Preparation of Palbociclib polymers based nanoparticles:

Palbociclib-loaded polymeric nanoparticles were prepared using a modified solvent evaporation method coupled with ionic gelatin. Chitosan (63.34 mg) was dissolved in 10 mL of 1% (v/v) acetic acid under magnetic stirring at 800 rpm and 25 ± 2 °C until a clear, homogeneous solution was obtained. Polyvinyl alcohol (PVA, 19.99 mg) was separately dissolved in distilled water at 70 °C, cooled to room temperature, and used as a stabilizing agent.

Folic acid (FA, 10 mg) was added to the chitosan solution, and the mixture was stirred at 600 rpm at room temperature for 2 h to ensure uniform polymer hydration and effective FA interaction with the chitosan matrix, thereby enabling ligand-mediated targeting. Palbociclib (75 mg) was dissolved in acetone, and the organic phase was then added dropwise to an aqueous solution of chitosan, FA, and PVA while stirring at 1000 rpm, forming an oil-in-water emulsion.

The resultant emulsion was stirred at 800 rpm for 4 h at 25°C to allow solvent evaporation and the formation of drug-loaded nanoparticles. Ionic gelatin was then added to the emulsion dropwise at 500 rpm with the TPP solution (0.5ml) to induce electrostatic cross-linking between chitosan and TPP, yielding a stable nanomatrix. The nanoparticle dispersion was adjusted with distilled water, stirred for 30 minutes, then centrifuged at 15,000 rpm for 30 minutes at 4°C to collect and wash the nanoparticles, which were then stored at 4°C for further analysis

[18], [24]. The detailed composition of the formulation is shown in Table 1.

Table 1: List of Composition of Palbociclib Nanoparticles

Ingredients	Amount
Palbociclib	75mg
Chitosan	63.34mg
Polyvinyl Alcohol	19.99mg
Folic Acid	10mg
Sodium tripolyphosphate (TPP) solution	2mg
Acetic Acid	10ml
Dist. Water	20ml

Characterization of Nanoparticles

A Zetasizer (Nano ZS90) was used to measure NP sizes, zeta potentials, and polydispersity indices, with the average of three readings. Particle size was calculated using dynamic light scattering (DLS), and zeta potential was assessed via electrophoretic mobility, which depends on the movement of particles under an electric field [18][19].

Drug Loading and Entrapment Efficiency

Quantitative estimation of polymeric nanoparticle drug loading (DL) and entrapment efficiency (EE) was performed using an indirect method for quantifying palbociclib. To do this, the nanoparticle suspension was centrifuged at a speed of 15,000 rounds per minute (rpm) for 30 minutes at a temperature of 4 °C to separate the pellet from the supernatant with the encapsulated drug. After collecting the supernatant containing the free drug, it was filtered through a 0.22 µm membrane and then analyzed by UV–visible spectrophotometry at 342 nm. The drug amount was determined using the established calibration curve. However, the nanoparticle pellet was washed with triple-distilled water and then lyophilized to determine the weight of the drug-loaded nanoparticles [19], [20]. The entrapment efficiency and drug loading were calculated using the following formulas.

$$\%\ \boldsymbol{Drug\ loading} = \frac{\boldsymbol{weight\ of\ drugs\ in\ NPs}}{\boldsymbol{weight\ of\ NPs}} \times \mathbf{100}$$

$$\%\boldsymbol{EE} = \frac{(\boldsymbol{Total\ drug\ in\ PNS - free\ drug})}{\boldsymbol{Total\ drug\ in\ formula}} \times \mathbf{100}$$

***In-vitro* Drug Release Studies**

This experiment evaluated the *in vitro* drug release of Palbociclib from nanoparticles in PBS (pH 7.4) and K acetate buffer (pH 5.4), using PLB release analysis via dialysis bag diffusion. Nanoparticles containing PB (15mg) were placed in a dialysis bag (1 kDa, LA387), which was then placed in a graduated bottle and surrounded by 100 mL of release medium. The complete system was operated at 37 ± 5°C with a stirrer speed of 100 rpm to maintain medium homogeneity. At each predetermined sampling time point from the receiver compartment, the same volume of fresh releaser medium was replaced [19].

Stability Study

Stability testing was performed in accordance with the ICH Q1A(R2) guidelines for new drug products. The lyophilized nanoparticle samples were packed in laminated aluminum foil pouches and stored under the following conditions:

Room temperature: 25 ± 2°C/60 ± 5% RH. Samples were collected at 0, 1, 2, and 3 months for evaluation [21], [24].

Antioxidant activity by using DPPH

The antioxidant potential of palbociclib polymeric nanoparticles was assessed using the DPPH radical-scavenging assay, with ascorbic acid as the reference standard. The test samples (PNs and ascorbic acid) were prepared in methanol at concentrations of 0.25, 0.5, and 1 µg/ml. Each sample (3 ml) was allowed to react with the 5 ml of 0.2mM methanolic DPPH for 30 minutes in the dark, after which the sample was measured spectrophotometrically at 342 nm[22]. The radical scavenging activity was calculated using the formula:

$$\%\ \boldsymbol{inhibition} = \frac{(\mathbf{Control\ absorbance - Test\ sample\ absorbanc})}{\mathbf{Control\ absorbance}} \times \mathbf{100}$$

***In-vitro* anti-inflammatory activity by the protein denaturation method**

The protein denaturation assay, used to establish the in vitro anti-inflammatory activity of palbociclib polymeric nanoparticles, was performed. Diclofenac was taken as the positive control. The samples of palbociclib, its nanoformulation, and diclofenac were used at experimental concentrations. Ranging from 10-160 µg/ml. Each time, it was incubated in phosphate-buffered saline, egg albumin was added, and the mixture was incubated at 27°C, followed by heating at 70°C to induce denaturation. The absorbance at 342 nm was measured after sufficient time had elapsed for the sample to cool [23]. Anti-inflammatory activity was calculated as a percentage inhibition relative to a control using the formula:

$$\%\ \boldsymbol{inhibition} = \frac{(\mathbf{Control\ absorbance\ -\ Test\ sample\ absorbance})}{\mathbf{Control\ absorbance}} \times \mathbf{100}$$

MTT assay by MCF-7

The cytotoxicity of the samples was determined on the MCF-7 (Immortal human cells derived from a cervical cancer, procured from NCCS Pune) cell line using the MTT Assay. Cells (10,000 cells/well) were plated in 96-well plates and incubated for 24 h in DMEM supplemented with 10% FBS and 1% antibiotic solution at 37°C with 5% CO_2. The next day, the cells were treated with different concentrations of the formulations (which were prepared in incomplete medium) and kept for incubation in the CO_2 incubator for 24 hours. Stock solutions of the samples were prepared in DMSO and subsequently diluted to obtain different concentrations in incomplete Cell culture Medium (Without FBS). This was followed by 24 h of incubation, after which MTT solution was added, and the optical density at 540 nm was measured in an iMark ELISA plate reader (IC50, calculated and reported below). Images of the treated cells were acquired using an inverted microscope (Olympus EK2) with a 10 MP Aptima CMOS camera (AmScope). IC50 was expressed as Mean ± SEM (Standard Error of Mean)[10]. The statistical significance of the results was evaluated by a one-way ANOVA test (statistical method), which was conducted in the software, GraphPad, version 8.

RESULT AND DISCUSSION

Selection of Wavelength

A 100 µg/ml solution of Palbociclib was scanned between 200 and 400nm to determine λmax using a double-beam UV Spectrophotometer (Shimadzu UV-1900). The absorption peak obtained from the experiment is shown in Figure 1. The maximum light absorption of Palbociclib at 342nm led to the selection of this wavelength for subsequent studies.

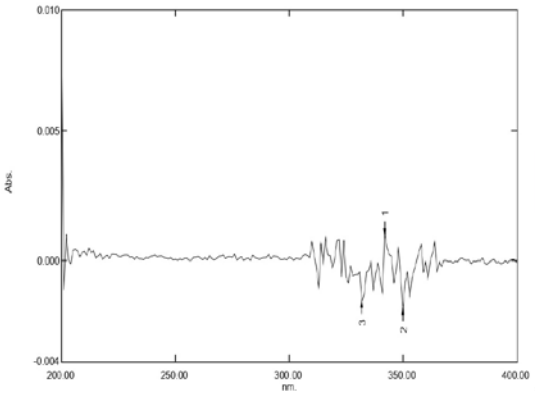

Figure 1: UV Spectrum of Palbociclib

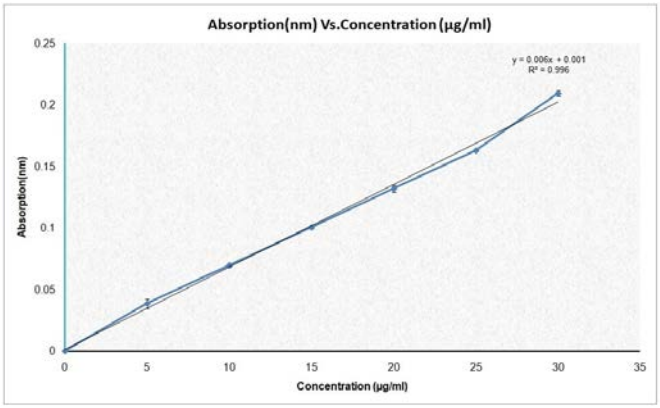

Figure 2: Standard curve of Palbociclib

Preparation of the Standard curve of Palbociclib

A calibration curve was constructed by plotting absorbance on the abscissa and concentration on the ordinate over the range 5–40 µg/ml. The plot showed a linear relationship (R^2 = 0.997), confirming that the compound obeyed the Beer–Lambert law, as shown in Figure 2.

Drug Excipients Interaction

FT-IR spectra have confirmed the structural stability of palbociclib and that it is consistent with the formulation excipients. The (Figure 3A) only palbociclib has displayed the N-H stretching (3400-3300 cm^{-1}), the aromatic & aliphatic C-H stretching (3060-2850 cm^{-1}), as well as, the most noticeable C=O/C =N stretching of the heterocyclic moiety (1650-1600cm^{-1}) bands; and the fact that the fingerprints also had the aromatic C=C and C-N vibrations assured the chemical identity of palbociclib**.** The FT-IR spectrum of the palbociclib–excipients mixture (Figure 3B) preserved distinctive drug peaks. Only slight band broadening was observed in the 3500–3200 cm^{-1} region due to the overlap of the O-H & N-H stretching vibrations of chitosan & PVA. The swings at 1650-1550cm^{-1} were a mix of palbociclib carbonyl & chitosan amide vibrations, whereas the polymer-specific C-O-C & C-O stretches emerged at around 1150 & 1050cm^{-1}. No new peaks or significant shifts were detected, indicating no chemical interactions. Minor spectral differences indicate weak hydrogen bonding, implying chemical stability of palbociclib and its miscibility with the selected excipients, making it suitable for polymeric nanoparticle formulation.

Role of folic acid as a targeting ligand

Using UV–Visible and FT-IR spectroscopy, the study clarified the role of folic acid (FA) as a targeting ligand in the palbociclib-loaded chitosan nanoparticle system. The investigation revealed that the UV–Vis spectra (Figure 4) of the FA-containing nanoparticles exhibited a sharp absorption peak at 280–290 nm, characteristic of the π→π* electronic transition of the pterin ring of FA. The persistence of the same absorbance bands and the

absence of major shifts indicate that FA retained its chemical structure and was not altered during nanoparticle formation. It is of utmost importance that the pterin moiety, which acts as an active receptor site for the folate receptors, is preserved; thereby showing that FA is still a ligand in the formulation.

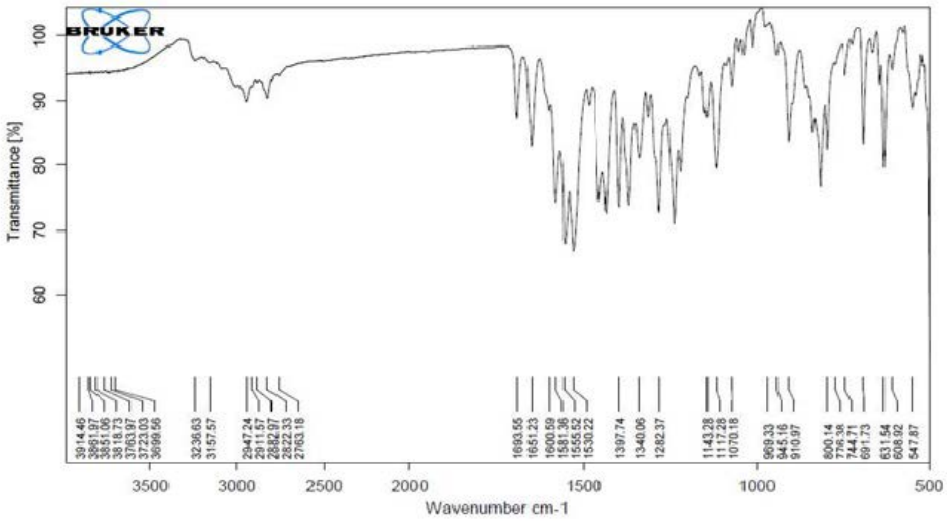

Figure 3A: FT-IR spectra of palbociclib

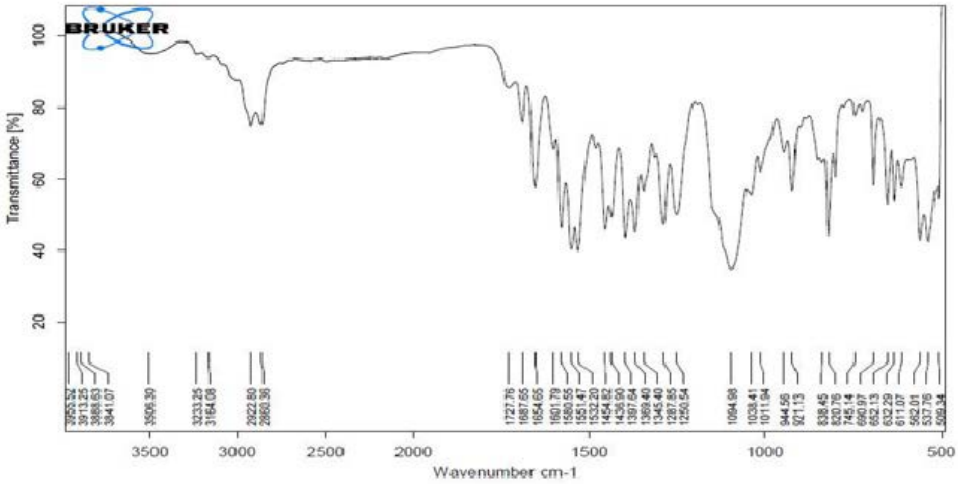

Figure 3B: FT-IR spectra of Palbociclib with the excipients

FT-IR spectroscopy analysis (Figure 5) further confirmed the presence of FA and provided insight into its behaviour within the chitosan-based nanoparticle matrix. The FT-IR spectrum of FA nanoparticles displayed characteristic bands at 3300–3400 cm^{-1} corresponding to O–H and N–H stretching vibrations, around 1700 cm^{-1} for the carboxyl C=O stretch, and within the 1600–1400 cm^{-1} range for C=C and C–N vibrational modes. The O–H/N–H stretching vibrational region considerably broadened, and the carboxyl C=O band weakened with a slight shift, supporting the argument for the presence of both hydrogen bonding and electrostatic interactions that are typical of the carboxylate groups of the FA and the protonated amino groups of the chitosan involved. A significant observation is that signals like the new amide I (~1650 cm^{-1}) and amide II (~1550 cm^{-1}) are absent, indicating that covalent amide bonds have not formed. These data conclusively demonstrate that FA is associated with nanoparticle surfaces via noncovalent interactions, thereby maintaining structural integrity and supporting its potential as an ideal ligand for cell-targeted therapy via the folate receptor.

Particles size and PDI

Particle size is one essential parameter for nanoparticle characterization. Particle size analysis of the prepared Palbociclib nanoparticles was done by using a Malvern Zeta Sizer. The analysis results showed that the nanoparticles had an average size of 237.8±1.76 nm, a Polydispersity Index (PDI) of 0.221 & an intercept value of 0.799. The zeta size distribution of the Palbociclib nanoparticles is shown in Figure 6a.

Particles Charge

Zeta potential was measured using a Malvern Zetasizer to quantify the particles' surface charge. The greater the surface charge, the more stable the material during storage. The magnitude of the zeta potential is an important predictor of colloidal stability; generally, zeta potentials of ±25 mV or higher indicate good stability. The zeta potential of the Palbociclib polymeric nanoparticles was +34.09 ± 3.38 mV, with 100% peak intensity. Hence, these Palbociclib polymeric nanoparticles exhibit excellent stability. Zeta potential distribution of the Palbociclib polymeric nanoparticles is shown in Figure 6b.

Drug loading and entrapment Efficiency

Palbociclib-polymeric nanoparticles exhibited high drug loading and entrapment efficiency, indicating effective encapsulation within the polymer matrix, as shown in Table 2.

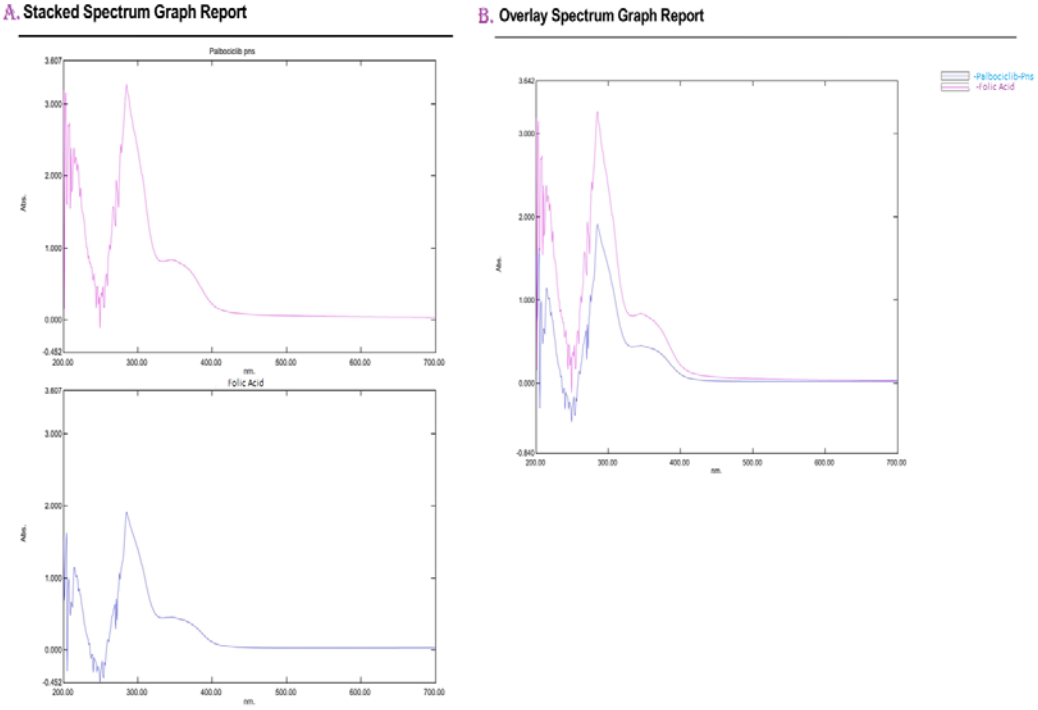

Figure 4: UV-Visible spectroscopic analysis of folic acid and folic acid-associated palbociclib Nanoparticle

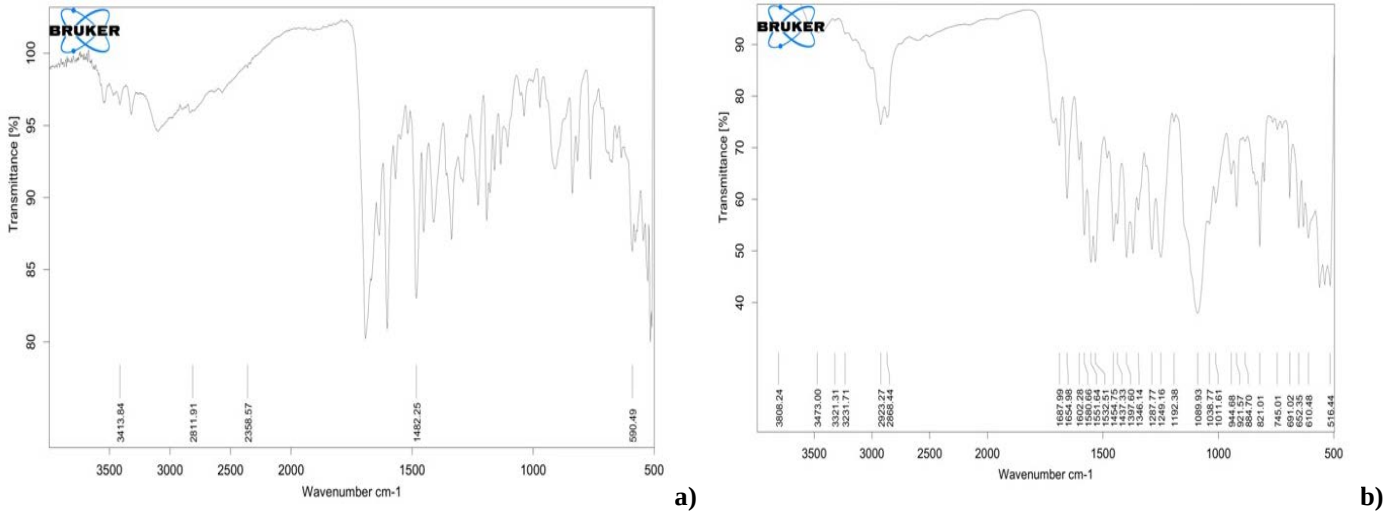

a) **b)**

Figure 5: FT-IR spectra of a) folic acid and b) folic acid-associated palbociclib Nanoparticle

Table 2: Result of Drug loading and entrapment Efficiency of optimized batch

Entrapment Efficiency (%)				Drug loading (%)			
Reading I	**Reading II**	**Reading III**	**Mean± SD**	**Reading I**	**Reading II**	**Reading III**	**Mean ± SD**
81.28	79.37	82.98	81.21±1.80	42.96	40.38	39.05	40.79±1.98

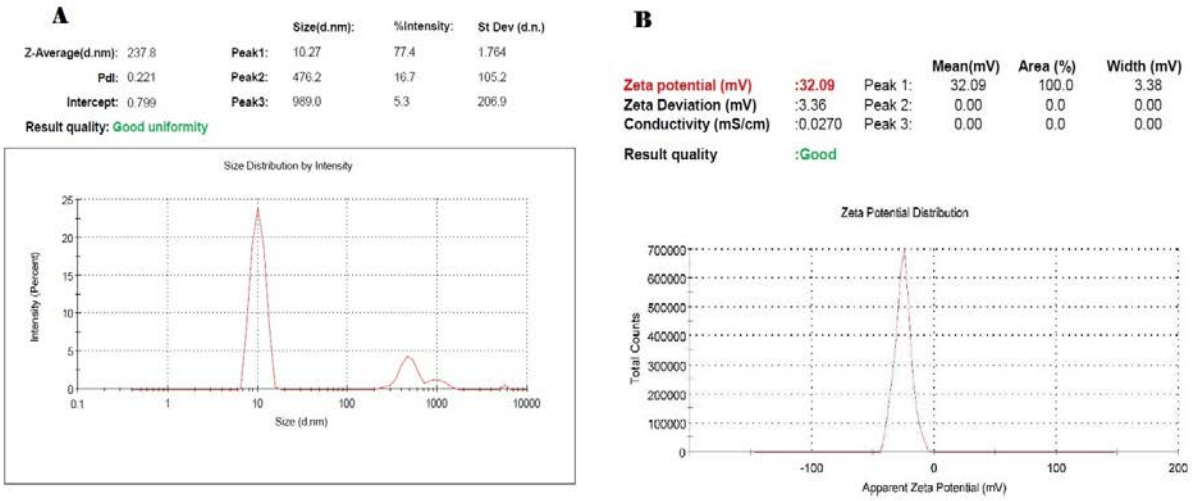

Figure 6: (A) Particle size of formulated palbociclib PNs (B): Particle charge of formulated palbociclib Polymeric nanoparticles

In-vitro drug release Profile

The *in vitro* release profile of palbociclib (PB) from the fabricated polymeric nanoparticles (PNs) was investigated under physiological sink conditions (37 ± 0.5 °C, 100 rpm) using a dialysis bag diffusion method. To simulate different biological environments, the release medium was varied between phosphate-buffered saline (PBS, pH 7.4) and potassium acetate buffer (pH 5.4). The purpose was to evaluate the release kinetics and the pH response of the formulation. As Figure 7 demonstrates, the formulation with PLB-loaded PNs exhibited a biphasic, long-lived release profile, as previously observed, and drug release increased with increasing pH. It was evident that drug release was markedly higher under acidic conditions (pH 5.4) than under neutral physiological conditions (pH 7.4) throughout the entire measurement period. For instance, the percentages reached 55.60 ± 0.89 and 93.25 ± 0.95 at 8 and 24 h, respectively, at pH 5.4. By contrast, at pH 7.4, nearly half of these percentages were achieved by 8 h (35.85 ± 1.02%), and the values increased to 80.78 ± 1.51% by 24 h. Disregarding time ($p < 0.0001$) and pH ($p < 0.0001$) as statistically significant, the two-way ANOVA of the release data indicated that both were critical and influenced cumulative drug release. The analysis further revealed that the two parameters, time and pH, interacted significantly ($p < 0.0001$). As a result, the interaction indicates that the release profiles at the two pH values are not parallel; the cumulative release gap between pH 5.4 and pH 7.4 widens with time, consistent with the dynamic, pH-triggered release of the nanoparticles. The observed release kinetics indeed serve the purpose of tumor-targeted therapy. The process in which the drug is released at a moderate rate at the blood's baseline pH is expected to reduce the risk of premature drug leakage and, hence, off-target toxicity. The release rate into the acidic tumor environment and acidic intracellular compartments is increased by the harshness of the tumor environment and by acidic intracellular compartments, which occurs after nanoparticle ingestion via endocytic receptors. The pH-dependent "stimulated release" increases locally and is achieved only by cancer cells, thereby inhibiting cell proliferation.

DPPH antioxidant activity

The DPPH assay results showed that the standard ascorbic acid exhibited the highest antioxidant activity (IC_{50} = 0.447 µg/ml; Table 3). Palbociclib PNs had almost the same ability of radical scavenging (IC_{50} = 0.52 µg/ml) as the standard, while the free palbociclib showed much less activity (IC_{50} = 2.041 µg/ml). The data suggest that nanoparticle encapsulation significantly enhances the antioxidant properties of palbociclib relative to the free form.

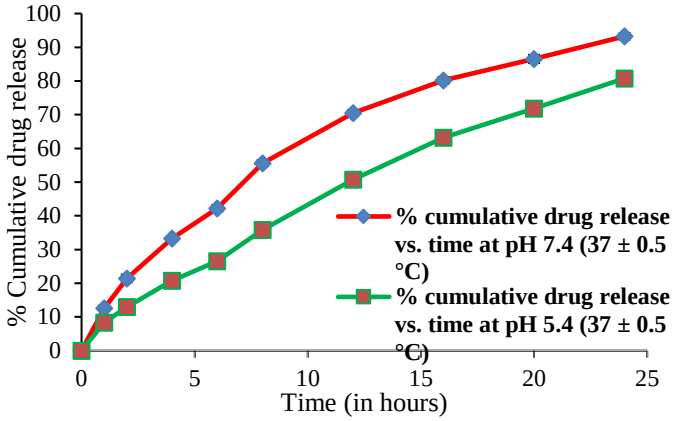

Figure 7: *In vitro* cumulative release of palbociclib from polymeric nanoparticles at pH 5.4 and 7.4 over time (24 hours) at 37°C with continuous agitation. Data is shown as mean ± SD (n=3).

Table 3: List of DPPH free radical scavenging of palbociclib PNS and palbociclib free drug

SN	Conc. (µg/ml)	%Inhibition		
		Ascorbic acid	Palbociclib PNs	Palbociclib –Free Drug
1	0.25	41.32 ± 1.4	26.71± 1.4	14.98± 1.4
2	0.5	52.34 ±0.9	49.71± 1.2	27.32±1.7
3	1.5	65.35 ±1.23	64.23± 1.6	40.92± 1.8
4	2.0	67.45±1.5	79.02± 1.4	49.43±1.7
5	2.5	76.35± 1.7	84.37± 1.2	56.4±2.1
IC50		**0.447 µg/ml**	**0.52µg/ml**	**2.041µg/ml**

***In-vitro* anti-inflammatory activity by protein denaturation method**

The protein denaturation assay results revealed a clear gradient in anti-inflammatory efficacy, as shown in Table 4. The most potent compound was the reference drug, diclofenac sodium, with an IC_{50} of 30.56 µg/ml. The palbociclib polymeric nanoparticles exhibited a moderate, statistically significant inhibitory effect, with an IC_{50} of 38.9 µg/ml. On the other hand, the Free Palbociclib was the weakest active agent, with an IC_{50} of 137.87 µg/ml.

Stability Profiling

Particle Size and Particle Charge Evaluation

DLS was used to analyze palbociclib-loaded chitosan nanoparticles to assess their stability during storage. The analysis included particle size, polydispersity index, and zeta potential at the start and three months later (Figure 8). The average particle size increased slightly from 237.80 ± 1.76 nm to 240.14 ± 1.91 nm (Figure 9), indicating storage without substantial aggregation. The PDI increased slightly from 0.221 to 0.283; however, it remains below the critical threshold of 0.3 and thus supports homogeneity of size. In addition, a slight decrease in zeta potential was noticed, i.e., +32.09 ± 3.36 mV to +30.01 ± 2.68 mV (Figure 10), but the surface charge was still enough for colloidal stabilization. A statistically significant interaction between storage time and nanoparticle characteristics ($p < 0.0001$) was revealed by two-way ANOVA ($\alpha = 0.05$). The variation between row and column (factors) accounted for 94.40% and 4.43% of the total variance, respectively. Thus, these results collectively confirm that the nanoparticles are physically and chemically stable during storage.

Table 4: List of Inhibition of Protein Denaturation of Palbociclib PNs

SN	Conc (µg/ml)	% Inhibition		
		Diclofenac sodium	Palbociclib PNs	Palbociclib Free drug
1	**10**	17.89 ± 1.6	12.76±2.6	8.9 ± 1.9
2	**20**	34.76 ± 1.8	25.87± 1.5	15.67 ± 1.8
3	**40**	54.73 ± 1.2	44.71±1.2	25.14 ± 1.3
4	**80**	78.98 ±1.3	68.6 ±1.3	38.82 ±1.7
5	**160**	88.59 ±0.9	83.34 ±1.2	54.23± 1.9
IC_{50}		**30.56 µg/ml**	**38.9 µg/ml**	**137.87µg/ml**

Drug loading (%)

Chitosan nanoparticles loaded with palbociclib exhibited sustained efficacy over the 1-year observation period. Initially, the mean drug load was 43.0% ± 1.64%, which went down just a bit to 40.1% ± 1.58% during the last month, with a total decline of around 6.7% from the starting level, demonstrating a nanoformulation that is very consistent with the drug content still being kept in a good state. A two-way ANOVA ($\alpha = 0.05$) indicated that storage time (the Row Factor) was the main, statistically significant source of variation ($p < 0.0001$), accounting for 94.40% of the overall variation. The contributions of experimental replication (the Column Factor) and the interaction of time and replication were also statistically significant but in opposite directions, accounting for 4.43% and 1.08% of the variation, respectively. The findings support the conclusion that the slight time-based reduction in drug loading quantifies formulation erosion, and that the formulation's overall stability remains strong (Figure 11a).

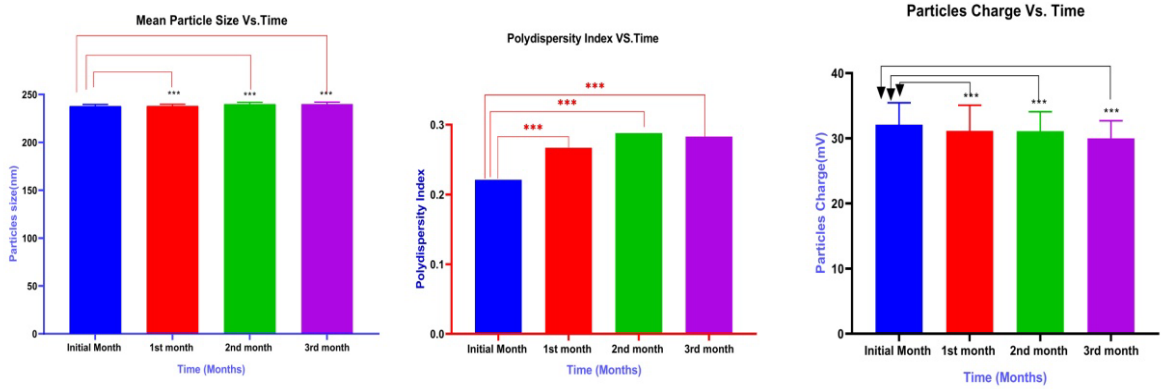

Figure 8: Storage stability of palbociclib-loaded PNs in terms of: (A) Mean particle size; (B) polydispersity index (PDI); and (C) Mean surface charge at baseline and after three months of storage. The data are presented as mean ± SD (n = 3). A significant interaction between storage time and nanoparticle characteristics was observed in the two-way ANOVA ($p < 0.0001$).

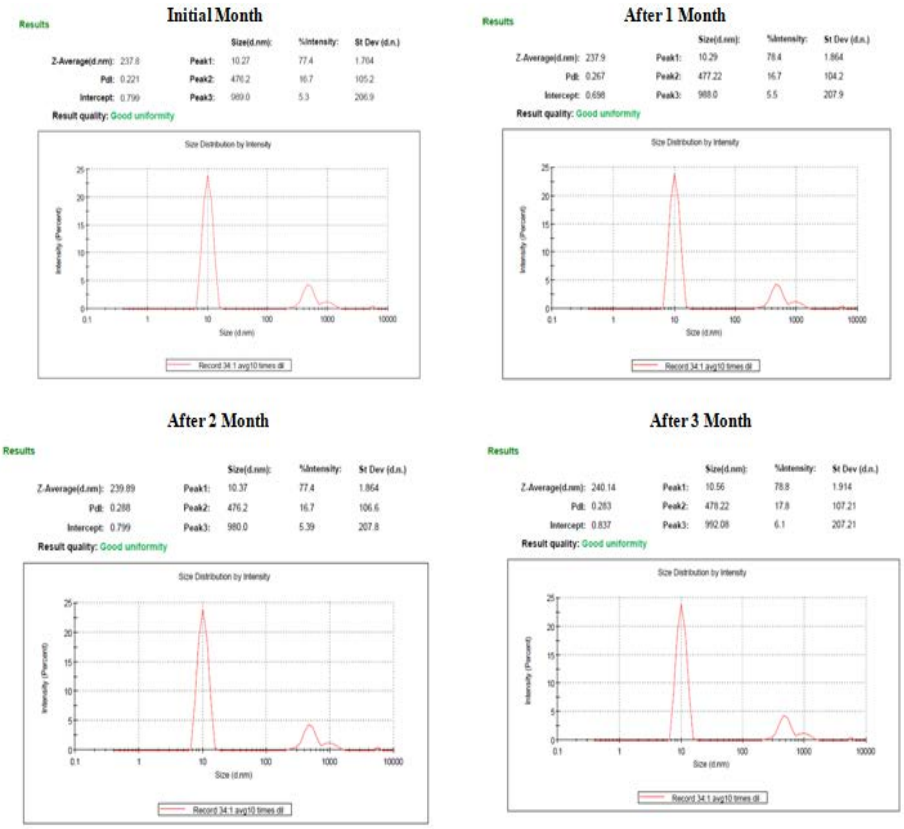

Figure 9: Dynamic light scattering (DLS) measurements report of palbociclib-loaded chitosan nanoparticles, the mean particle size at the start (0 months) and after three months of storage

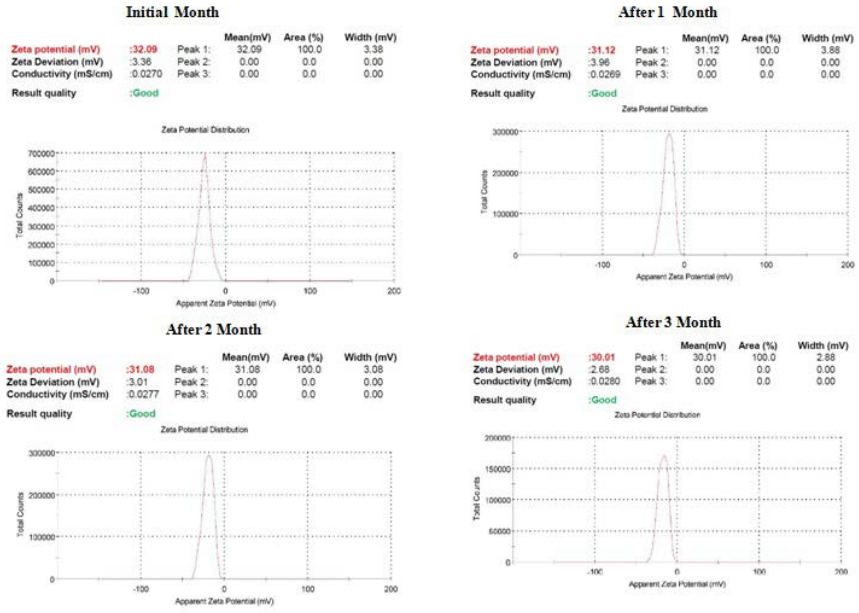

Figure 10: Dynamic light scattering (DLS) measurements report of palbociclib-loaded chitosan nanoparticles, the mean particle charge (mV) at the start (0 months) and after three months of storage

Entrapment Efficiency

The prepared chitosan nanoparticle formulation demonstrated high initial entrapment efficiency for palbociclib, which was well preserved throughout the three-month stability assessment. As summarized in (Figure 11b), the first level of entrapment efficiency was 81.28 ± 2.56% (mean ± SD, n = 3), showing that the inclusion of palbociclib was very successful in the chitosan nanomatrix. After storage, the decrease was very small, with entrapment efficiency remaining at 79.02 ± 2.69% after three months. This indicates that the difference relative to the initial

value is very small, approximately 2.8%, reflecting the formulation's storage stability and the very good retention of the encapsulated drug. The entrapment efficiency was analyzed using a two-way ANOVA ($\alpha = 0.05$) with storage time as the row factor and batch as the column factor. The column factor (batch variation) was found to be significant and the source of variation ($p < 0.0001$) at 99.98% total (pure) variation. Conversely, neither storage time (row factor; p=0.9898) nor their interaction (p=0.2296) was significant in terms of statistical reference. In other words, the marginal changes in entrapment efficiency across storage periods were random, and the efficiency still mapped onto approximately the same plane rather than being systematically invariant.

MTT assay

The result of the MTT assay carried out on MCF-7 breast cancer cells indicated that Palbociclib-loaded polymeric nanoparticles (PB-PNs) showed (Figure 12) a more effective cytotoxicity than the free Palbociclib. The IC_{50} value of the PB-PNs was 5.85 µg/ml, which is approximately 3.1-fold lower than that of the reference Palbociclib (18.15 µg/ml), indicating that anticancer potency is enhanced at a lower dose. PB-PNs perform better in this regard through nanoencapsulation, which increases cellular uptake via endocytosis, enhances drug stability, and enables slow release, resulting in higher intracellular drug accumulation. In contrast, free Palbociclib was less effective and may have been degraded due to low uptake.

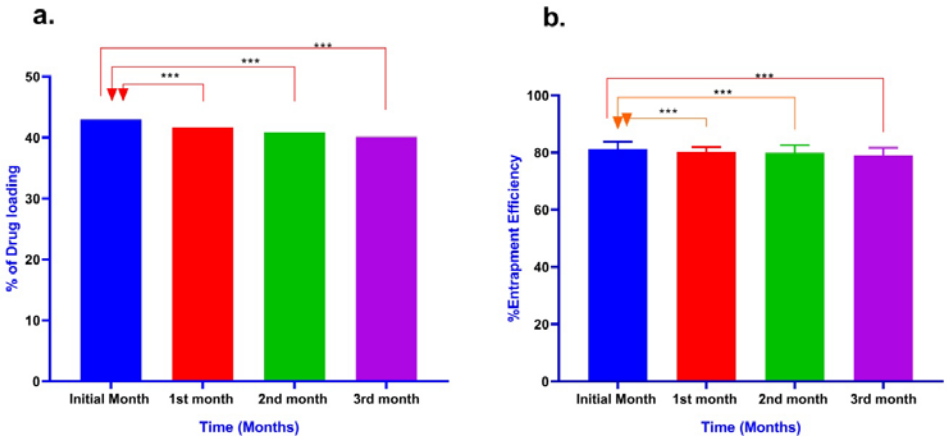

Figure 11: Stability of palbociclib-loaded chitosan nanoparticles stored for three months. (A) Stability of drug loading expressed as mean ± SD (n = 3); two-way ANOVA revealed a significant impact of storage time ($p < 0.0001$). (B) Entrapment efficiency during storage is presented as mean ± SD (n = 3). A two-way ANOVA showed no significant effect of storage time ($p > 0.05$), confirming the stability of encapsulation.

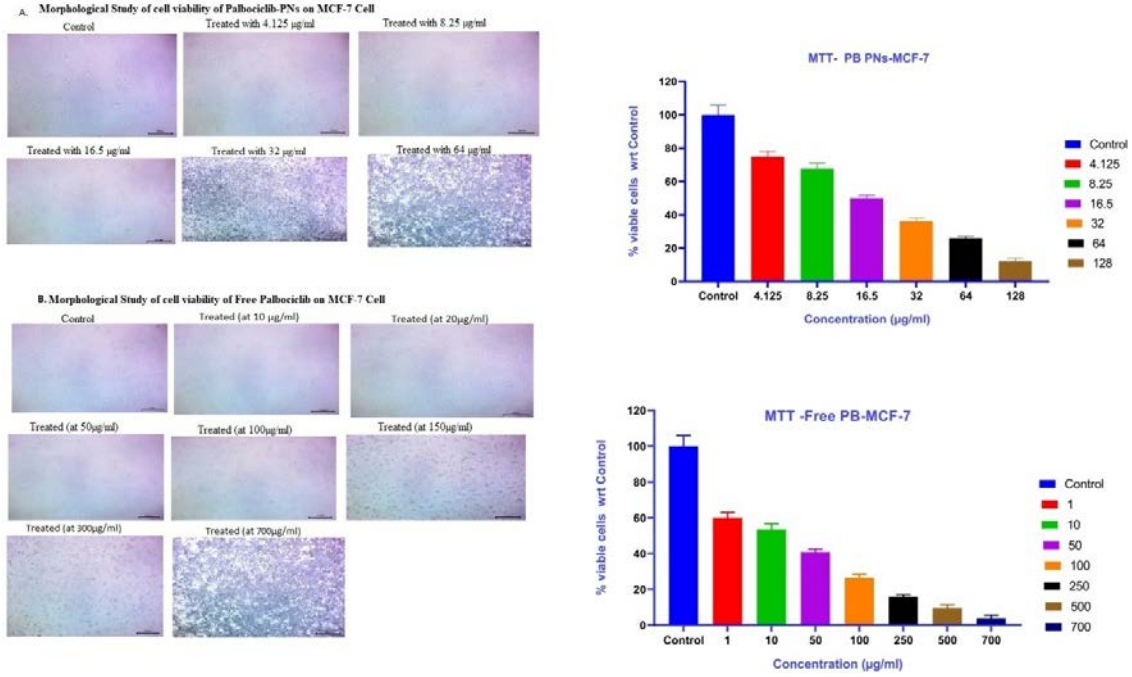

Figure 12: Comparative cytotoxicity of Palbociclib-loaded polymeric nanoparticles (PB-PNs) and free Palbociclib against MCF-7 breast cancer cells as determined by the MTT assay

DISCUSSION

Current work focused on the synthesis and characterization of Palbociclib-loaded polymeric nanoparticles (PLB-loaded PNs), which serve as carriers for Palbociclib (PB), a cyclin-dependent kinase (CDK) 4/6 inhibitor. Various analytical and cell biological studies have confirmed that the formulation is already in place, owing to its versatility, stability, and capacity to enhance the therapeutic window. UV-spectrophotometric studies showed a peak at 342 nm (λmax) for the drug, which was used in all subsequent analyses. The standard curve was linear (R^2 = 0.997) over the concentration range 5–40 µg/ml, supporting the applicability of Beer's law and enabling future concentration determinations in further studies. Moreover, FT-IR studies of physical blends revealed no interaction between PLB and the selected excipients, indicating good compatibility between the drug and the formulation. The role of folic acid as a targeting ligand was confirmed by using both UV–Visible and FT-IR spectroscopic methods. The UV–Visible spectra of folic acid-linked palbociclib nanoparticles presented a classical absorption border at 280–290 nm, which corresponded to π→π* electronic transitions taking place in the pterin ring of folic acid. No significant bathochromic or hypochromic shifts were observed, indicating that the folic acid molecule's chemical structure remained unchanged during the nanoparticle synthesis and that the pterin moiety was preserved. The latter is critical because the pterin moiety mediates folic acid binding to folate receptors, which are often overexpressed on cancer cells. FT-IR analysis also showed that folic acid was present in the chitosan nanoparticle matrix and interacted with it. O–H and N–H stretching (3300–3400 cm^{-1}), carboxyl C=O stretching (approximately 1700 cm^{-1} and C=C/C–N vibrations (1600–1400 cm^{-1}) were the characteristic bands identified. Since they were broadened or weakened, their positions were not moving, meaning that the O–H/N–H stretching mode was expanded. The carboxylate C=O band was slightly weakened, indicating hydrogen bonding and electrostatic interactions between the carboxylate groups of folic acid and the protonated amino groups of chitosan. The lack of any new peaks corresponding to the amide I (~1650 cm^{-1}) and amide II (~1550 cm^{-1}) FTIR bands confirmed that folic acid was bonded to the nanoparticle surface through non-covalent bonds instead of covalent conjugation.

This noncovalent bonding strategy maintained the ligand's bioactivity. Favorable physicochemical characterization of PLB-loaded PNs for favorable drug delivery was observed. For passive targeting, the particles are measured at 237.8 ± 1.76 nm (PDI = 0.221), with a monodisperse size distribution that approaches or falls within the flotation range due to the EPR effect. The PB-loaded PN has a high zeta potential positive value of (+34.09 mV), meaning that an opposing charge repels each particle, creating the likelihood of high-colloidal stabilization and aggregation resistance, both in storage and in biologic systems. This is supported by an elevated entrapment efficiency (81.21 ± 1.80%) and drug loading (40.79 ± 1.98%), thereby indicating optimal encapsulation. Drug release profiles of the drug *in vitro* demonstrated dependence on pH conditions and a sustained release nature side by side. The higher release at pH 5.4 (93.25% in 24 h) compared with pH 7.4 (80.78%) is a strategically useful feature for drug-release studies. pH-dependent release from this type of chitosan complex formulation minimizes drug leakage into the systemic circulation at pH ~7.4, thereby reducing adverse effects. On the other hand, an accelerated release at the acidic root environment better accommodates the tumor microenvironment and endo-lysosomal compartments, thereby facilitating drug release specifically within cancer cells and enhancing therapeutic efficacy at the site of action. An effect size indicates a strong and significant interaction ($p < 0.0001$), suggesting that the time × pH interaction is a consistent characteristic of the formulation.

Apart from the determinable primary functions of anticancer activity, the PB-PNs (IC_{50} = 0.52µg/ml) had acceptable additional pharmacological properties. Specifically, the DPPH antioxidant assays confirmed that. In contrast, the nanoformulation significantly reduced the IC_{50} for self-protection against oxidative stress, substantially outperforming free PLB (IC_{50} = 2.041 µg/ml) and ascorbic acid. Likewise, PB-PNs (IC_{50} = 38.9 µg/ml) showed more efficient in vitro anti-inflammatory activity than the bulk drug (IC_{50} = 137.87 µg/ml). This enhancement may be due to increased solubility and bioavailability conferred by nanoencapsulation, which could confer selective benefits for any treatment against inflammatory states commonly linked to cancer progression. The long-term stability of the formulation was evidenced by the fact that no parameter changed over 3 months. Hence, we conclude that the particle size, PDI, zeta potential, drug loading, and entrapment efficiency of the formulation were not affected when held constant. The slight increase in size (up to 240.14 nm) and PDI (up to 0.283), while zeta potential gradually decreased (to +30.01 mV), were statistically and practically insignificant in

suggesting any instability. The high retention of the drug content (≈93.3% of the initial loading after 3 months) further supports its stability. The MTT assay performed on MCF-7 breast cancer cells indicated that Palbociclib-loaded polymeric nanoparticles (PB-PNs) exhibited greater cytotoxicity than free Palbociclib. The IC_{50} value of the PB-PNs was 5.85 µg/ml, which is approximately 3.1-fold lower than that of the reference Palbociclib (18.15 µg/ml), indicating that anticancer potency is enhanced at a lower dose. PB-PNs perform better in this regard through nanoencapsulation, which increases cellular uptake via endocytosis, enhances drug stability, and enables slow release, resulting in higher intracellular drug accumulation. In contrast, free Palbociclib was less effective and may have been degraded due to low uptake.

CONCLUSION

This study focused on developing and characterizing Palbociclib-loaded polymeric nanoparticles (PLB-loaded PNs) as targeted drug delivery systems for cancer treatment. Analytical techniques confirmed the stability, compatibility, and non-covalent binding of folic acid as a targeting ligand, and that it remains functional for receptor-mediated uptake. The nanoparticles exhibited favorable physicochemical properties, including approximately spherical morphology, high zeta potential, and high drug entrapment efficiency, supporting their potential for passive targeting via the EPR effect. Release studies demonstrated pH-dependent, sustained drug release that favors tumor microenvironments while minimizing systemic leakage. Additional pharmacological benefits included enhanced antioxidant and anti-inflammatory effects relative to free Palbociclib, attributable to improved solubility and bioavailability achieved by nanoencapsulation. The formulation remained stable for three months, with minimal changes in parameters. Cytotoxicity assays on MCF-7 breast cancer cells revealed a significantly higher potency of the nanoformulation, with lower IC_{50} values indicating enhanced efficacy through improved cellular uptake, stability, and controlled-release mechanisms. Overall, the nanoparticle system shows promise as an effective, stable, and targeted delivery platform for Palbociclib in cancer therapy.

FINANCIAL ASSISTANCE

NIL

CONFLICT OF INTEREST

The authors declare no conflict of interest.

AUTHOR CONTRIBUTION

Nurjamal Hoque contributed to conceptualization, Formal Analysis, Methodology, investigation, resources, visualization, and writing the original draft. Ananta Choudhury contributed to funding acquisition, methodology, project administration, software, supervision, manuscript review, and editing.

REFERENCES

[1] Waks AG, Winer EP. Breast Cancer Treatment. *JAMA*, **321**, 288 (2019) https://doi.org/10.1001/jama.2018.19323

[2] Britt KL, Cuzick J, Phillips K-A. Key steps for effective breast cancer prevention. *Nat Rev Cancer*, **20**, 417–36 (2020) https://doi.org/10.1038/s41568-020-0266-x

[3] Vemuri SK, Banala RR, Mukherjee S, Uppula P, S GPV, GR AV, M T. Novel biosynthesized gold nanoparticles as anti-cancer agents against breast cancer: Synthesis, biological evaluation, molecular modelling studies. *Mater Sci Eng C*, **99**, 417–29 (2019) https://doi.org/10.1016/j.msec.2019.01.123

[4] Gomathi AC, Xavier Rajarathinam SR, Mohammed Sadiq A, Rajeshkumar S. Anticancer activity of silver nanoparticles synthesized using aqueous fruit shell extract of Tamarindus indica on MCF-7 human breast cancer cell line. *J Drug Deliv Sci Technol*, **55**, 101376 (2020) https://doi.org/10.1016/j.jddst.2019.101376

[5] Mirza Z, Karim S. Nanoparticles-based drug delivery and gene therapy for breast cancer: Recent advancements and future challenges. *Semin Cancer Biol*, **69**, 226–37 (2021) https://doi.org/10.1016/j.semcancer.2019.10.020

[6] Zhang W, Hong C, Pan C. Polymerization-induced self-assembly of functionalized block copolymer nanoparticles and their application in drug delivery. *Macromol Rapid Commun*, **40**, (2019) https://doi.org/10.1002/marc.201800279

[7] Sur S, Rathore A, Dave V, Reddy KR, Chouhan RS, Sadhu V. Recent developments in functionalized polymer nanoparticles for efficient drug delivery systems. *Nano-Struct Nano-Objects*, **20**, 100397 (2019) https://doi.org/10.1016/j.nanoso.2019.100397

[8] Rajan M, Murugan M, Ponnamma D, Sadasivuni KK, Munusamy MA. Poly-carboxylic acids functionalized chitosan nanocarriers for controlled and targeted anti-cancer drug delivery. *Biomed Pharmacother*, **83**, 201–11 (2016) https://doi.org/10.1016/j.biopha.2016.06.026

[9] Rocca A, Schirone A, Maltoni R, Bravaccini S, Cecconetto L, Farolfi A, Bronte G, Andreis D. Progress with palbociclib in breast cancer: latest evidence and clinical considerations. *Ther Adv Med Oncol*, **9**, 83–105 (2017) https://doi.org/10.1177/1758834016677961

[10] Chen T, Xing F, Sun Y. Facile fabrication of TPGS-PCL polymeric nanoparticles for paclitaxel delivery to breast cancer: investigation of antiproliferation and apoptosis induction. *J Exp*

Nanoscience, **19**, (2024) https://doi.org/10.1080/17458080.2023.2281938

[11] Farhat F, Tarabaih M, Kanj A, Aoun M, Kattan J, Assi T, Awada A. Palbociclib safety and efficacy beyond ribociclib-induced liver toxicity in metastatic hormone-receptor positive breast cancer patient. *Anti-Cancer Drugs*, **31**, 85–89 (2020) https://doi.org/10.1097/CAD.0000000000000845

[12] Niehemann K, Schneider SW, Luger TA, Godin B, Ferrari M, Fuchs H. Nanomedicine—challenge and perspectives. *Angew Chem Int Ed*, **48**, 872–97 (2009) https://doi.org/10.1002/anie.200802585

[13] Dikpati A, Di Maio V, Ates E, Greffard K, Bertrand N. Studying the stability of polymer nanoparticles by size exclusion chromatography of radioactive polymers. *J Control Release*, **369**, 394–403 (2024) https://doi.org/10.1016/j.jconrel.2024.03.053

[14] Presas E, Sultan E, Gervasi V, Crean AM, Werner U, Bazile D, O'Driscoll CM. Long-term stability of insulin glulisine loaded nanoparticles formulated using an amphiphilic cyclodextrin and designed for intestinal delivery. *Drug Dev Ind Pharm*, **46**, 1073–9 (2020) https://doi.org/10.1080/03639045.2020.1775631

[15] Bott RF, Oliveira WP. Storage conditions for stability testing of pharmaceuticals in hot and humid regions. *Drug Dev Ind Pharm*, **33**, 393–401 (2007) https://doi.org/10.1080/03639045.2020.1775631

[16] Muthu MS, Feng S-S. Pharmaceutical stability aspects of nanomedicines. *Nanomedicine*, **4**, 857–60 (2009) https://doi.org/10.2217/nnm.09.75

[17] Krishnakumar N, Sulfikkarali N, RajendraPrasad N, Karthikeyan S. Enhanced anticancer activity of naringenin-loaded nanoparticles in human cervical (HeLa) cancer cells. *Biomed Prev Nutr*, **1(4)**, 223–231 (2011) https://doi.org/10.1016/j.bionut.2011.09.003

[18] Schaffazick SR, Pohlmann AR, Dalla-Costa T, Guterres SS. Freeze-drying polymeric colloidal suspensions: nanocapsules, nanospheres and nanodispersion. A comparative study. *Eur J Pharm Biopharm*, **56**, 501–5 (2003) https://doi.org/10.1016/S0939-6411(03)00139-5

[19] Yang C-R, Zhao X-L, Hu H-Y, Li K-X, Sun X, Li L, Chen D-W. Preparation, optimization and characteristic of huperzine A loaded nanostructured lipid carriers. *Chem Pharm Bull*, **58**, 656–61 (2010) https://doi.org/10.1248/cpb.58.656

[20] Mandal B, Bhattacharjee H, Mittal N, Sah H, Balabathula P, Thoma LA, Wood GC. Core–shell-type lipid–polymer hybrid nanoparticles as a drug delivery platform. *Nanomedicine*, **9**, 474–91 (2013) https://doi.org/10.1016/j.nano.2012.11.010

[21] Lemoine D, Francois C, Kedzierewicz F, Preat V, Hoffman M, Maincent P. Stability study of nanoparticles of poly(ε-caprolactone), poly(d,l-lactide) and poly(d,l-lactide-co-glycolide). *Biomaterials*, **17**, 2191–7 (1996) https://doi.org/10.13040/IJPSR.0975-8232.13(3).1241-50

[22] Valko M, Leibfritz D, Moncol J, Cronin MTD, Mazur M, Telser J. Free radicals and antioxidants in normal physiological functions and human disease. *Int J Biochem Cell Biol*, **39**, 44–84 (2007) https://doi.org/10.1016/0142-9612(96)00049-X

[23] Yadav R, Mahalwal DVS. In-vitro anti-inflammatory activity of oral poly herbal formulations. *Pharma Innov J*, **7**, 272–6 (2018) http://dx.doi.org/10.1016/j.biocel.2006.07.001

[24] Hoque N, Choudhury A, Datta D. Formulation, central composite design optimization and in vitro evaluation of folic acid conjugated palbociclib loaded polymeric nanoparticles. *J Young Pharm*, **17**, 877–86 (2025) https://dx.doi.org/10.5530/jyp.20250155